

Curvature Estimation over Smooth Polygonal Meshes using The Half Tube Formula

Ronen Lev¹, Emil Saucan², and Gershon Elber³

¹ OptiTex Ltd., Petach-Tikva 49221, Israel, ronen.lev@optitex.com

² Electrical Engineering Department, Technion, Haifa 32000, Israel,
semil@ee.technion.ac.il

³ Computer Science Department, Technion, Haifa 32000, Israel,
gershon@cs.technion.ac.il

Abstract

The interest, in recent years, in the geometric processing of polygonal meshes, has spawned a whole range of algorithms to estimate curvature properties over smooth polygonal meshes. Being a discrete approximation of a C^2 continuous surface, these methods attempt to estimate the curvature properties of the original surface. The best known methods are quite effective in estimating the total or Gaussian curvature but less so in estimating the mean curvature.

In this work, we present a scheme to accurately estimate the mean curvature of smooth polygonal meshes using a one sided tube formula [16] of the volume above the surface. In the presented comparison, the proposed scheme yielded results whose accuracy is amongst the highest compared to similar techniques for estimating the mean curvature.

1 Introduction

Polygonal meshes are basic representations of geometry that are employed in a whole variety of fields from vision and image processing to computer graphics, geometric modeling and manufacturing. Analysis of such data sets is of great value in many applications such as reconstruction, segmentation and recognition or even non photorealistic rendering. In this context, curvature analysis plays a major role. As an example, curvature analysis of 3D scanned data sets were shown to be one of the best approaches to segmenting the data [32].

Though many algorithms attempt to estimate the total, or Gaussian curvature K , and mean curvature, H , of the original surface, given its polygonal approximation, we will discuss here only the most well known and accurate ones. For a more rigorous comparison of curvature estimation methods, see, for example, [28].

In [17, 26], the principal curvatures and principal directions of a triangulated surface are estimated at each vertex by a least square fitting of an osculating paraboloid to the vertex and its neighbors. These references use quadratic approximation methods where the approximated surface is obtained by solving an over-determined system of linear equations.

In [23], one can find an asymptotic analysis of the paraboloid fitting scheme and an algorithm based on the Gauss-Bonnet Theorem [11], which we refer to as the Gauss-Bonnet scheme, that also known as the *angle deficit* method [23]. In [6, 12], the angular deficiency around a vertex is used to estimate the total curvature at a vertex. In a planar domain, the angles around a vertex sums to 2π . The deviation from this value directly reflects on the total curvature at the vertex. A similar estimation is derived for the mean curvature, this time through the dihedral angle of the incoming edges to the vertex.

In [22], circular cross sections, near the examined vertex, are fitted to the surface. Then, the principal curvatures are computed using Meusnier's and Euler's theorems (see [11]). In [29], the principal curvatures are estimated with the aid of an eigenvalues/vectors analysis of 3×3 symmetric matrices that are defined via an integral formulation. In [30], the fact that $\frac{1}{2\pi} \int_0^{2\pi} k_n(\varphi) d\varphi = H$ and $\frac{1}{2\pi} \int_0^{2\pi} k_n(\varphi)^2 d\varphi = \frac{3}{2}H^2 - \frac{1}{2}K$, where $k_n(\varphi)$ is the normal curvature in direction φ , is used to estimate K and H , via discrete approximations of these integrals around a vertex.

In this work, we present a curvature estimation scheme that exploits an infinitesimal volume above the piecewise linear surface to estimate both the total, Gaussian curvature K , and the mean curvature H . It will be shown that this volume above the surface is related to both H as a second order term and to K as a third order term. This identity is then exploited to estimate H accurately and to a lesser extent, K . Further, it will be shown that this formulation is similar to the one offered in [6, 12] for the estimation of K and H while more precise results are achieved here for H .

The rest of this paper is organized as follows. In Section 2, we discuss related work and provide the background that is necessary for the proposed algorithm and present the half tube formula. In Section 3, we present the proposed algorithm for the discrete, polygonal case. Then, in Section 4, we provide some examples and compare our results to other curvature estimation algorithms. We summarize our results in Section 5, and give some possible directions for further research.

2 Background and Related Work

Let $S \subset \mathbb{R}^3$ be an orientable surface and let \bar{N}_p denote the unit normal of S at p . For each $p \in S$ consider, in the direction of \bar{N}_p , the open symmetric interval of length $2\varepsilon_p$, I_{p,ε_p} , where ε_p is chosen to be small enough such that $I_{p,\varepsilon_p} \cap I_{q,\varepsilon_q} = \emptyset$, for any $p, q \in S$ such that $\|p - q\| > \xi \in \mathbb{R}_+$. Then, $Tub_\varepsilon(S) = \bigcup_{p \in S} I_{p,\varepsilon_p}$ is an open set that contains S and such that for any point $x \in Tub_\varepsilon(S)$, there exists a unique normal line to S through x . $Tub_\varepsilon(S)$ is called a *tubular neighborhood* of S

or just a *tube*; See Figure 1. The two surfaces $S_{\pm\epsilon} = S \pm \epsilon\bar{N}$ are called the *offset surfaces* of S with offset distance ϵ . We shall consider sets of constant offset ϵ .

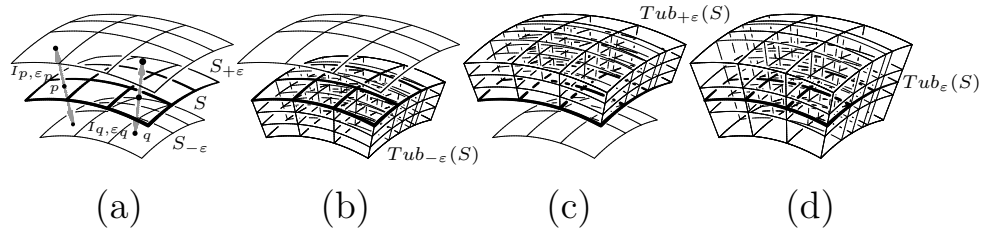


Fig. 1. Tubular neighborhood of S .

Note that, since ϵ_p depends upon p , $Tub_{\epsilon}(S)$ does not, in general, coincide with the ϵ -neighbourhood of S , i.e., with the set $N_{\epsilon}(S) = \{x \in \mathbb{R}^3 \mid dist(x, S) = \epsilon\}$. Also, it is important to know that, while not evident, the existence of tubular neighborhoods is assured both locally, for any regular, orientable surface (see [11], Proposition 1, p. 111), and globally for regular, compact, orientable surfaces (see [11], Proposition 3, p. 113).

In addition, we note a number of facts about the existence and regularity of the offset surface S_{ϵ} : If S is convex, then $S_{\pm\epsilon}$ are piecewise $\mathcal{C}^{1,1}$ surfaces (i.e., they admit parameterizations with continuous and bounded derivatives), for all $\epsilon > 0$. Also, if S is a smooth enough surface with a boundary (that is, at least piecewise \mathcal{C}^2), then $S_{\pm\epsilon}$ are piecewise \mathcal{C}^2 surfaces, for all small enough ϵ (see [13], p. 1025). Moreover, for any compact set $S \subset \mathbb{R}^3$, $S_{\pm\epsilon}$ are Lipschitz surfaces for almost any ϵ (see [18]). This is extremely pertinent to our study, since it allows the computation of the mean curvature for local triangulations, not only for smooth surfaces (see also the discussion in Section 5 below).

Theorem 1. (The Tube Formula) *Let $S \subset \mathbb{R}^3$ be a compact orientable surface. Then*

$$Vol(Tub_{\epsilon}(S)) = 2\epsilon Area(S) + \frac{2\epsilon^3}{3} \int_S K dA. \quad (1)$$

Proof: Following [16]. Let $S = f(U)$ be a local parametrization of the surface. Define $f_{\delta} : U \rightarrow \mathbb{R}^3$, $f_{\delta}(u, v) = f(u, v) + \delta\bar{N}(u, v)$. Then, for a sufficiently small $|\delta|$, f_{δ} is injective, for all $|\epsilon| < |\delta|$. Thus, one can choose ϵ such that $f_{\pm\epsilon}$ represents a parametrization of $S_{\pm\epsilon}$.

Then:

$$\begin{cases} \frac{\partial f_{\epsilon}}{\partial u} = \frac{\partial f}{\partial u} + \epsilon \frac{\partial \bar{N}}{\partial u}, \\ \frac{\partial f_{\epsilon}}{\partial v} = \frac{\partial f}{\partial v} + \epsilon \frac{\partial \bar{N}}{\partial v}. \end{cases} \quad (2)$$

However, $II_S(\bar{w}) = -d\bar{N} \cdot \bar{w}$, where II_S denotes the second fundamental form of S (see [11], p. 141). Thus, one can express the partial derivatives of f_{ϵ} as:

$$\begin{cases} II_S \frac{\partial f}{\partial u} = -\frac{\partial \bar{N}}{\partial u}, \\ II_S \frac{\partial f}{\partial v} = -\frac{\partial \bar{N}}{\partial v}. \end{cases}$$

Therefore (2.2) becomes:

$$\begin{cases} \frac{\partial f_\varepsilon}{\partial u} = (1 - \varepsilon II_S) \frac{\partial f}{\partial u}, \\ \frac{\partial f_\varepsilon}{\partial v} = (1 - \varepsilon II_S) \frac{\partial f}{\partial v}, \end{cases} \quad (3)$$

and

$$\frac{\partial f_\varepsilon}{\partial u} \times \frac{\partial f_\varepsilon}{\partial v} = \det(1 - \varepsilon II_S) \left(\frac{\partial f}{\partial u} \times \frac{\partial f}{\partial v} \right).$$

Moreover, $\det(1 + \varepsilon I_S) > 0$, for small enough ε , thus

$$\left\| \frac{\partial f_\varepsilon}{\partial u} \times \frac{\partial f_\varepsilon}{\partial v} \right\| = \det(1 - \varepsilon II_S) \left\| \frac{\partial f}{\partial u} \times \frac{\partial f}{\partial v} \right\|.$$

From the classical formula expressing the principal curvatures of S in terms of H and K (see [11], p. 212, [24], pp. 208-9):

$$\det(1 - \varepsilon II_S) = 1 - 2\varepsilon H + \varepsilon^2 K,$$

it follows (by the well known differential geometry expression for area – see, e.g., [11], 2-8.) that:

$$\begin{aligned} Area(f_\varepsilon(U)) &= \int_U \left\| \frac{\partial f_\varepsilon}{\partial u} \times \frac{\partial f_\varepsilon}{\partial v} \right\| dudv \\ &= \int_U (1 - 2\varepsilon H + \varepsilon^2 K) \left\| \frac{\partial f}{\partial u} \times \frac{\partial f}{\partial v} \right\| dudv \\ &= Area(f(U)) - 2\varepsilon \int_{f(U)} H dA + \varepsilon^2 \int_{f(U)} K dA. \end{aligned}$$

Thus, by summation over the local parameterizations composing S ,

$$Area(S_{\pm\varepsilon}) = Area(S) \mp 2\varepsilon \int_S H dA + \varepsilon^2 \int_S K dA. \quad (4)$$

Therefore, $Area(S_{+\varepsilon}) + Area(S_{-\varepsilon}) = 2Area(S) + 2\varepsilon^2 \int_S K dA$, and follows that:

$$Vol(Tub_\varepsilon(S)) = \int_{-\varepsilon}^{+\varepsilon} Area(S_t) dt = 2\varepsilon Area(S) + \frac{2\varepsilon^3}{3} \int_S K dA,$$

whence (2.1) follows immediately.

By applying the Gauss-Bonnet Theorem for compact surfaces (see [11], p. 276), one immediately gets the following corollary:

Corollary 1. *Let $S \subset \mathbb{R}^3$ be a compact orientable surface. Then:*

$$\text{Vol}(\text{Tub}_\varepsilon(S)) = 2\varepsilon \text{Area}(S) + \frac{4\pi\varepsilon^3}{3} \chi(S), \quad (5)$$

where $\chi(S)$ denotes the Euler characteristic of S .

Evidently, the Tube Formula can not be employed to compute the mean curvature. Moreover, in the case of triangulated surfaces computing K by means of the Tube Formula reduces to approximating $K(p)$ by the angle defect at the point p (see [9], p. 9 and Remark 1 below); i.e., by approximating $K(p)$ by $K(p) = 2\pi - \sum_j \psi_j$, where ψ_j denote the angles of the triangles incident with p (see Figure 4) – that is, by applying a well known method, based upon the Local Gauss-Bonnet Theorem (see [6], [21]). Fortunately, (1) also yields a much more useful (yet generally overlooked) formula, which we will refer to as the Half Tube Formula:

Theorem 2. (Half Tube Formula) *Let $S \subset \mathbb{R}^3$ be a compact orientable surface. Then*

$$\text{Vol}(\text{Tub}_{\pm\varepsilon}(S)) = \varepsilon \text{Area}(S) \mp \varepsilon^2 \int_S H dA + \frac{\varepsilon^3}{3} \int_S K dA. \quad (6)$$

Remark 1. A similar formula is developed in [9], p. 4, for *full* tubes, without, however, noticing that the term containing H vanishes. Indeed, our method is closely related to that of [9]. However they stem from somewhat different considerations. Note that, as already mentioned above, only the use of the half tubes formula allows the computation of the mean curvature. Moreover, the method we propose has the advantage of being simpler to implement than the one proposed in [9].

3 The Algorithm

The tube formula is, in fact, a generalization of the classical Steiner-Minkowski Theorem ([2] 12.3.5, [16] Theorems 10.1 and 10.2.) for compact, convex polyhedra with non-empty interiors of dimension $n \geq 2$, which we present only in the relevant cases, $n = 2$ and $n = 3$:

Theorem 3. (Steiner-Minkowski) *Let $P \subset \mathbb{R}^n$, $n = 2, 3$ be a compact, convex polyhedron and let $N_\varepsilon(P) = \{x \in \mathbb{R}^n \mid \text{dist}(x, P) \leq \varepsilon\}$, $n = 2, 3$.*

1. *If $n = 2$, then,*

$$\text{Area}(N_\varepsilon(P)) = \text{Area}(P) + \varepsilon \text{Length}(\partial P) + \pi\varepsilon^2, \quad (7)$$

where ∂P denotes the boundary of P .

2. If $n = 3$, then,

$$Vol(N_\varepsilon(P)) = Vol(P) + \varepsilon Area(\partial_2 P) + C\varepsilon^2 Length(\partial_1 P) + \frac{4\pi\varepsilon^3}{3}, \quad (8)$$

where $\partial_2 P$ denotes the boundary faces of P , $\partial_1 P$ denotes the boundary edges of P and the last term contains the 0-dimensional volume contribution of the boundary vertices of P (by convention: $Vol(\partial_0 P) = |V_P|$ - the number of vertices of P), and where $C = C(P)$ is a scalar value that encapsulates $\iint_S H$ and that essentially depends on the dihedral angles of P .

To gain some insight, we start by analyzing the 2-dimensional case first. $N_\varepsilon(P)$ naturally decomposes into three components: P itself, a union of rectangles of height ε constructed upon the sides of P (see Figure 2) and the union of circular sectors of radius ε (see Figure 2 (a)). The total area of the rectangles is:

$$\varepsilon Length(e_1) + \dots + \varepsilon Length(e_n) = \varepsilon Length(\partial P),$$

where e_1, \dots, e_n denote the boundary edges of P . The angles ϕ_n of the circular sectors are given by: $\phi_i = 2\pi - \pi/2 - \pi/2 - \alpha_i = \pi - \alpha_i$, where α_i is the respective internal angle of P (see Figure 2 (a)). However, $\alpha_1 + \dots + \alpha_n = (n - 2)\pi$, thus $\phi_1 + \dots + \phi_n = 2\pi$. That is, the circular sectors combine to form a disk of radius ε (see Figure 2 (b)).

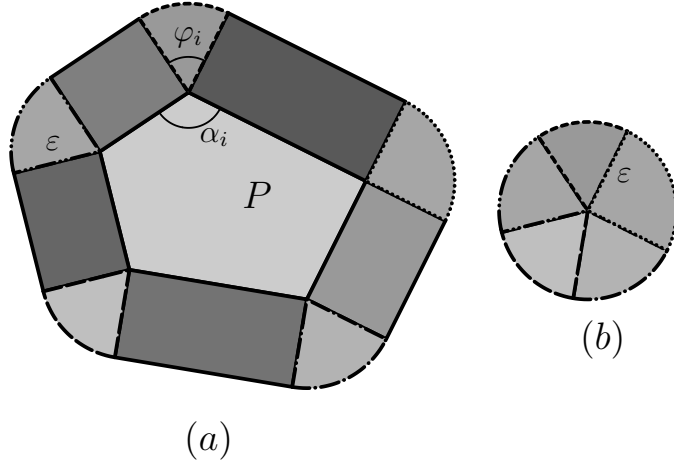


Fig. 2. Tubular neighborhood of a convex polygon.

In the case of $n = 3$, $N_\varepsilon(P)$ decomposes into the following four components: P , right parallelipeds \mathcal{P}_ε of height ε built upon the faces, the orthogonal products \mathcal{T}_ε of circular sectors and edges, and spherical sectors \mathcal{S}_ε associated with the vertices of P and whose union is a ball of radius ε (see Figure 3). Each of the

geometrical objects above gives rise to the terms of (3.2) containing the fitting power of ε .

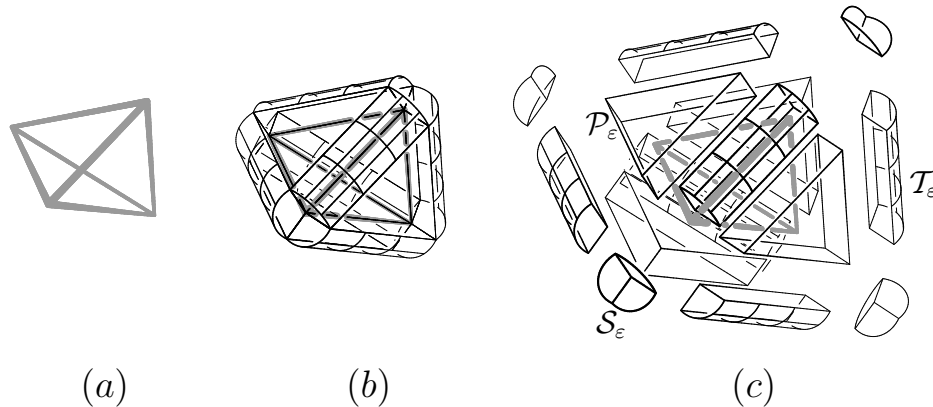


Fig. 3. Tubular neighborhood of convex polyhedron. Note the right parallelepipeds \mathcal{P}_ε built upon the faces, the orthogonal products \mathcal{T}_ε of circular sectors and edges, and spherical sectors \mathcal{S}_ε associated with the vertices.

One immediately notices the similarity between Formulas (2.4) and (3.2), more precisely the correspondence between the terms pertaining to H in both of the equations. Beyond its integral expression in (2.4), due to the limiting process possible on a smooth surface, the main difference resides in the “ \pm ” sign, sign due to discarding the overly restrictive convexity condition.

We denote by $H(p)$ and $K(p)$, the mean and Gauss curvatures at the point p , respectively. Before we proceed further we have to introduce the notion of convergence “in the sense of measures”. By convergence in the “sense of measures” we mean the following: given a patch U (i.e., several links of a certain vertex) on the triangulated surface S , each element in U (i.e., vertices, edges, etc.) makes a certain contribution to $H(K)$. Even if these contributions may not individually be correct, they do add to the correct answer *on the average*, when the density of the mesh increases. It is important to note that this averaging effect is not a local phenomenon.

It should be emphasized that while in the computation of $H(p)$, the dihedral angles of the edges through p , e_1, \dots, e_n (see Figure 4) are computed, this is done only in the sense of measures, this being true for the areas involved in expressing (in the expression of) $K(p)$ (see [15], [9]).

That is, one should regard, for instance, $Area(T_i)$ as a weight associated with the triangle T_i and uniformly distributed among its vertices p, q, r . The same uniform distribution is to be considered with respect to the weights naturally associated with edges. Therefore, the measure, i.e., of the dihedral angle

associated with the edge e_1 , for instance, is to be equally distributed among the vertices adjacent to it, i.e. p and q .

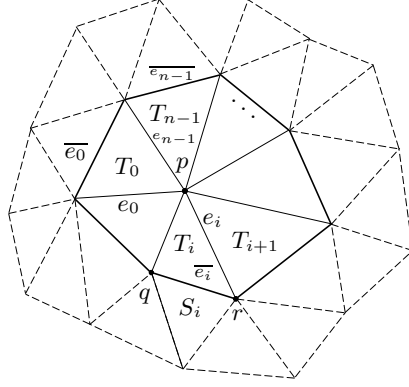


Fig. 4. The first ($Ring_1(p)$, solid) and second ($Ring_2(p)$, dashed) ring around vertex p .

The same type of uniform distribution is to be considered when computing the contribution of $Area(T_i)$, for example in the computation of $K(p)$: T_i will contribute $\frac{1}{3}Area(T_i)$ to the computation of (each of) $K(p), K(q), K(r)$ (see Figure 4 [27]).

However, the edge $\bar{e}_i = qr$ also contributes to $H(p)$, since it is an element of T_i , which is adjacent to p . (This may be counterintuitive to the classical approach of computing curvatures of curves *through* p , but one should remember that these “elementary” edge-curvatures are to be viewed as measures!) Since the boundary edge \bar{e}_i is common to T_i and the second-ring triangle S_i , its contribution to each of the T_i triangles is half of the associated dihedral angle. Analogous considerations are to be applied in computing the contribution of the boundary vertices (e.g., q), etc.

Let $Ring_i(p)$ be the i 'th ring around p and denote by $|e_i|$ the length of edge e_i . Then, the formula employed for computing the $H(p)$ follows:

$$H(p) = \frac{1}{Area(Ring_1(p))} \left[\frac{1}{2} \sum_{i=0}^{n-1} \varphi(T_i, T_{(i+1) \bmod n}) |e_i| + \frac{1}{4} \sum_{i=0}^{n-1} \varphi(T_i, S_i) |\bar{e}_i| \right],$$

where $S_i \in Ring_2(p)$ shares edge \bar{e}_i with $T_i \in Ring_1(p)$, and $\varphi(T_i, T_{i+1})$ denotes the dihedral angles between adjacent triangles T_i and T_{i+1} .

Algorithm 1 summarizes this process:

If the user requires the mean curvature for many vertices of the model, this algorithm can be implemented more efficiently as follows: First calculate the

Algorithm 1 Estimates the mean curvature at vertex p

```

RingArea  $\leftarrow$  0; ▷ The area of the first ring around vertex  $p$ 
ContribSum  $\leftarrow$  0; ▷ The sum of the contributions of the triangles from the first
ring around vertex  $p$ 
 $n \leftarrow |Ring_1(p)|$ ; ▷ Number of triangles in the first ring around vertex  $p$ 
for  $i \leftarrow 0$  to  $n - 1$  do
    RingArea  $+=$  Area( $T_i$ );
    ContribSum  $+=$   $\varphi(T_i, T_{(i+1) \bmod n})|e_i| + \frac{1}{2}\varphi(T_i, S_i)|\bar{e}_i|$ ;
end for
Return  $\frac{ContribSum}{2RingArea}$ ;

```

contribution of each edge. For each edge, e_i , that is adjacent to triangles T_i and T_{i+1} , we assign an attribute called *EdgeContrib* that is equal to $\frac{1}{4}\varphi(T_i, T_{i+1})|e|$. Then, for each triangle we assign an attribute called *TriangleContrib* that is the sum of all *EdgeContrib* of its' edges. Finally, we can compute the mean curvature at vertex p using Algorithm 2.

Algorithm 2 Estimates the mean curvature at vertex p . Efficient version.

```

RingArea  $\leftarrow$  0; ▷ The area of the first ring around vertex  $p$ 
ContribSum  $\leftarrow$  0; ▷ The sum of the contributions of the triangles from the first
ring around vertex  $p$ 
 $n \leftarrow |Ring_1(p)|$ ; ▷ Number of triangles in the first ring around vertex  $p$ 
for  $i \leftarrow 0$  to  $n - 1$  do
    RingArea  $+=$  Area( $T_i$ );
    ContribSum  $+=$   $T_i.TriangleContrib$ ;
end for
Return  $\frac{ContribSum}{2RingArea}$ ;

```

4 Tests and Examples

The algorithm described in Section 3 above was tested on a set of synthetic models representing the tessellations of five NURB surfaces: the body and the spout of the infamous “Utah teapot”, a hyperboloid, an ellipsoid and a torus. All these models along with their respective analytic curvature values for each vertex are also available in

http://www.cs.technion.ac.il/~gershon/poly_crvtr/.

The triangulations of each model were produced for a series of different resolutions, ranging from approximately one hundred triangles to several thousand triangles. Such a distribution of resolutions allowed us gain more insight into the convergence rate of the proposed algorithm and of the various comparison algorithms.

We considered the following mean error value (over all m vertices):

$$\frac{1}{m} \sum_{i=1}^m |H_i - \bar{H}_i|,$$

where H_i denotes the analytically computed value of the mean curvature from the smooth NURBs surface $S(r, t)$ at (r_i, s_i) and \bar{H}_i represents the value of the mean curvature that was estimated by one of the comparison methods at the triangular mesh vertex $v_i = S(r_i, t_i)$.

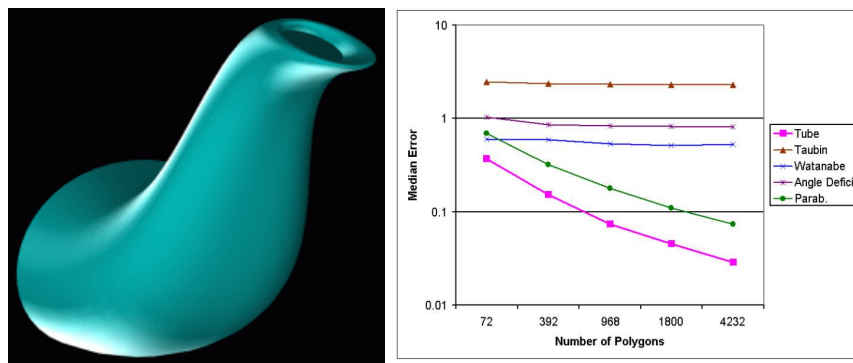


Fig. 5. Average of the absolute error for the value of mean curvature for the tessellations of the Utah teapot's body NURB surface.

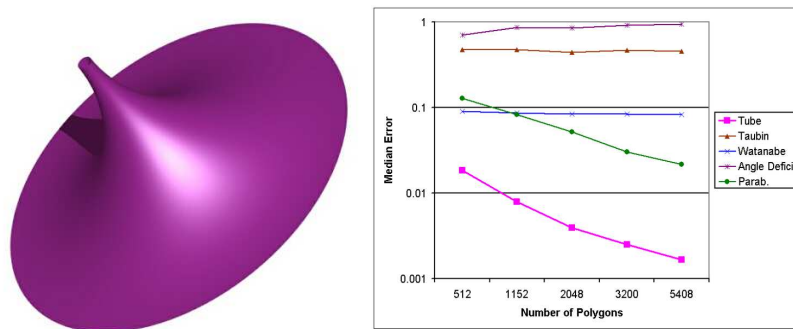


Fig. 6. Average of the absolute error for the value of mean curvature for the tessellations of a rotation surface of negative Gauss curvature.

We compared our algorithm's performance with that of the following previously tested ones: Gauss-Bonnet (or *angle deficit*) [6, 12, 23], Taubin [29], Watanabe [30] and the classical Parabolic Fit [17, 26].

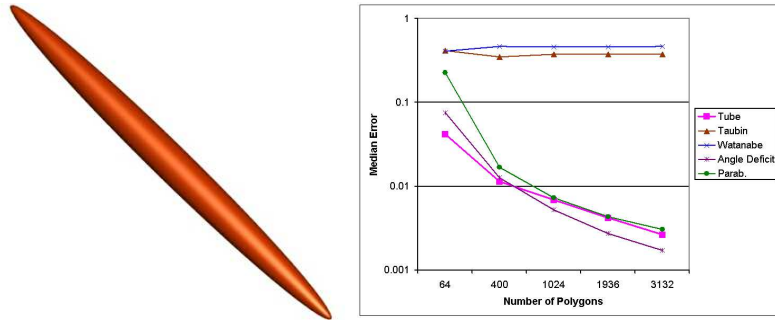


Fig. 7. Average of the absolute error for the value of mean curvature for the tessellations of the ellipsoid.

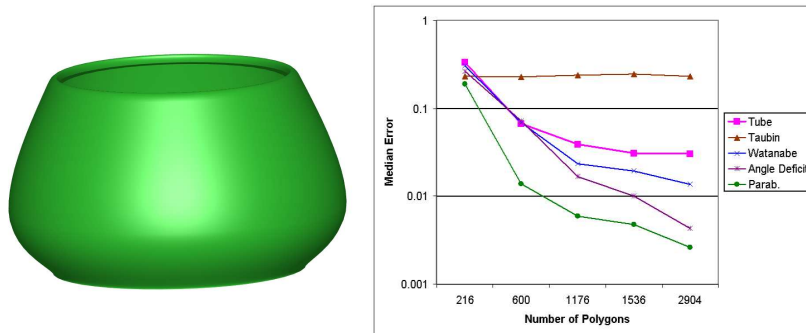


Fig. 8. Average of the absolute error for the value of mean curvature for the tessellations of the Utah teapot's body NURB surface.

It is evident from the graphs above that the Tube Formula method gives the best results among the methods (algorithms) for computing mean curvature, both on surfaces of negative Gauss curvature K (i.e., the hyperboloid) and on surfaces where K takes both positive and negative values (e.g., the spout and the torus). The results obtained when employing our method closely approach those obtained by the best method (e.g., the Parabolic Fit) in the case of surfaces of positive Gauss curvature of high variance (e.g., the ellipsoid).

It fails to produce very good results only for the Body. The probable reason that lays behind this failure is that, in the “middle section” of the Body, of almost zero Gauss curvature, the tessellation produces patches of (local) negative Gauss curvature, thus introducing the observed error in the computation of the mean curvature. This problem is currently under further investigation.

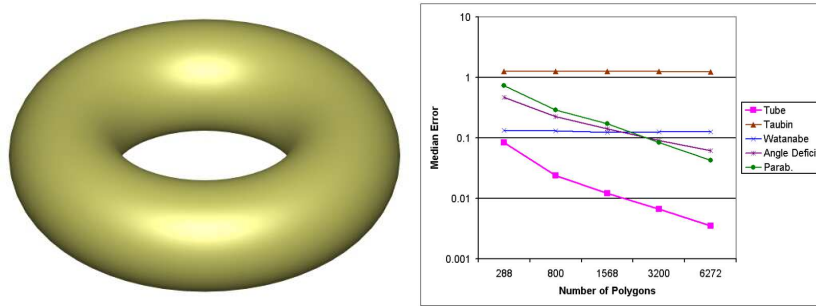


Fig. 9. Average of the absolute error for the value of mean curvature for the tessellations of the torus.

5 Conclusion and Future Work

As already noted above, it is evident that the Half-Tube Formula method produces, in general, good results, more so for surfaces of negative and mixed Gauss curvature. This is apparently due to the averaging effect of the tubes (or *normal cycles* ([9], [10], [15]), which represent a generalization of Steiner’s approach on convex polyhedra to a much larger class of geometrical objects, in particular to smooth and piecewise-linear manifolds in any dimension) above edges adjacent to vertices of negative curvature (see Figure 10).

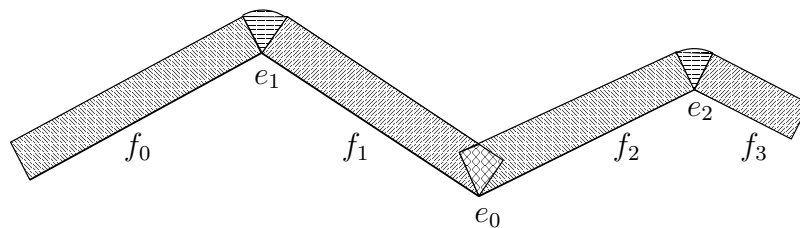


Fig. 10. Normal Cycle at Negative Curvature Vertex

Considering the quality results obtained in the case of mean curvature for most types of surfaces, and in light of Formulas (1) and (6), it is natural to next plan to investigate the capability (versatility, utility and potential) of the Tube and Half-Tube formulas in computing (approximating) K .

Another direction of study stems from the following facts: Both the Steiner-Minkowski Theorem and the Tube (and Half-Tube) Formula extend not only to arbitrary convex sets in \mathbb{R}^n (see [2]), but also to open subsets with compact closure with smooth boundary in any Riemannian manifold (see [16], pp. 10-11 and 243-248). The most straightforward generalization is the following theorem:

Theorem 4. (Weyl) (See [3], Theorem 6.9.9.) *If X is an k -dimensional sub-manifold of \mathbb{R}^n , then:*

$$Vol(Tub_\varepsilon(X)) = \sum_{i=0}^{\lfloor k/2 \rfloor} c_{2i} \varepsilon^{n-k+2i};$$

where

$$c_{2i} = \frac{1}{n-k+2i} \int_X K_{2i} dV_{2i},$$

and where K_{2i} are polynomials of degree i in the curvature tensor R of X , the so-called Weyl curvatures (see [3], [7]).

In particular, we have $c_0 = vol(X)vol(\mathbb{B}^{n-k}(0, \varepsilon))$ and $c_2 = \frac{1}{2} \int_X \kappa dX$, where κ denotes the *scalar curvature* (see [3], 6.9, [16], Lemma 4.2). It follows, that in the case of special interest for us, i.e., $n = 3$ and $k = 2$, we have: $Vol(Tub_\varepsilon(X)) = c_0\varepsilon + c_2\varepsilon^3$, where $\kappa \equiv K$ – the Gauss curvature of the surface X , i.e., we recover Formula (1).

Moreover, via the normal cycle the results above also extend to piecewise linear manifolds (piecewise linearly and isometrically) embedded in \mathbb{R}^n (see [8], [14], [9]). Recently these theorems were generalized to general closed sets in \mathbb{R}^n (see [19]).

This last fact is particularly important for the purpose of our study, since it allows us to apply the Half Tube Formula not only locally, that is by computing the measures associated with the triangles belonging to the ring of a given vertex p , but also to extend it to the next ring, and, potentially, to more consecutive rings. Moreover, since the Half Tube Formula involves K also, it allows us estimate K by computing over more than one ring, thus permitting the extension of the angle deficiency method to more than one ring. However, since by (6), the computation of K involves ε^3 , one expects difficulties to arise, due to numerical instability.

One further possible direction of investigation should be to answer the following (rather practical) question: Does the assumption regarding the uniform distribution of the area hold also for “bad” triangulations (i.e., containing “thin” triangles), and how much did it affect the quality of the mesh? In view of the seminal results of [7] regarding the good approximations of curvature measures for smooth manifolds by piecewise linear (PL) manifolds whose simplices are

“fat” (i.e., satisfy a certain non-degeneracy condition imposed upon the dihedral angles in all dimensions), one is inclined to conclude that “fat” triangles should be considered if one wants to make use of the uniform distribution of the area assumption, in which case the original question should be replaced by the more technical one: “What is the lower admissible boundary for the “fatness” of the triangles if a uniform distribution is to be considered?”

A direct application of our method would be in the computation for of *Willmore (elastic) energy* of triangulated surfaces, where the the Willmore $W(S)$ energy of be a smooth, compact surface S isometrically immersed in \mathbb{R}^3 is defined as:

$$W(S) = \int_S H^2 dA. \quad (9)$$

Our approach represents an alternative to the one proposed in [4]. Since the Willmore energy is a *conformal invariant* (see [31]), its computation is relevant in a variety of fields and their applications, such as in *conformal geometry, variational surface modeling, thin structures* (see [5]) and *medical imaging* (see [25]).

Another immediate use of our algorithm would be to compute the integral $\int_S H$. Since this integral is *bending invariant* [1], its computation may prove to be useful in applications involving *PL isometric embeddings* (see, e.g. [20]).

Acknowledgment

Emil Saucan is supported by the Viterbi Postdoctoral Fellowship. This work was partially supported by European FP6 NoE grant 506766 (AIM@SHAPE).

References

1. Almgren, F. J. and Rivin, I. The mean curvature integral is invariant under bending, The David Epstein 60th birthday Festschrift (I. Rivin, C. Rourke, C. Series, eds.), International Press 1999.
2. M. Berger, *Geometry II*, Universitext, Springer-Verlag, Berlin, 1987.
3. M. Berger and B. Gostiaux, *Differential Geometry: Manifolds, Curves and Surfaces*, Springer-Verlag, New York, 1987.
4. Bobenko, A. I. *A conformal energy for simplicial surfaces*, Combinatorial and Computational Geometry, MSRI Publications, vol. 52, 133-143, 2005.
5. Bobenko, A. I. and Schröder, P. *Discrete Willmore Flow*, Eurographics Symposium on Geometry Processing (Desbrun, M. and Pottman, H., eds.), 2005.
6. Borrelli, V., Cazals, F. and Morvan, J.-M. *On the angular defect of triangulations and the pointwise approximation of Curvatures*, Computer Aided Geometric Design 20, pp. 319-341, 2003.
7. Cheeger, J. Müller, W. and Schrader, R. *On the Curvature of Piecewise Flat Spaces*, Comm. Math. Phys. , 92, pp. 405-454, 1984.
8. Cheeger, J. Müller, W. and Schrader, R. *Kinematic and Tube Formulas for Piecewise Linear Spaces*, Indiana Univ. Math. J., 35 (4), pp. 737-754, 1986.
9. Cohen-Steiner, D. and Morvan, J. M. *Restricted Delaunay triangulations and normal cycle*. In Proc. 19th Annu. ACM Sympos. Comput. Geom., pp. 237–246, 2003.

10. Cohen-Steiner, D. and Morvan, J. M. *Approximation of Normal Cycles*, Research Report 4723, INRIA, 2003.
11. do Carmo, M. P. *Differential Geometry of Curves and Surfaces*, Prentice-Hall, Englewood Cliffs, N.J., 1976.
12. Dyn, N., Hormann, K., Kim, S.-J. and Levin, D. *Optimizing 3d triangulations using discrete curvature analysis*, (T. Lyche and L.L. Schumaker, eds.), Mathematical Methods in CAGD: Oslo 2000 Nashville, TN, 2001. Vanderbilt University Press, pp. 135-146, 2001.
13. Federer, H. *Curvature measures*, Trans. Amer. Math. Soc., 93, 418-491, 1959.
14. Flaherty, F. J. *Curvature measures for piecewise linear manifolds*, Bull. Amer. Math. Soc., 79(1), 100-102.
15. Fu, J. H. G. *Convergence of Curvatures in Secant Approximation*, J. Differential Geometry, 37, pp. 177-190, 1993.
16. Gray, A. *Tubes*, Addison-Wesley, Redwood City, Ca, 1990.
17. Hamann, B. Curvature approximation for triangulated surfaces. In *Computing Suppl.*, number 8, pages 139-153, 1993.
18. Howland, J. and Fu, J. H. G. *Tubular neighbourhoods in Euclidean spaces*, Duke Math. J., 52(4), 1025-1045, 1985.
19. Hug, D., Last, G. and Weil, W. *A local Steiner-type formula for general closed sets and applications*, Mathematische Zeitschrift, Vol.246, No. 1-2, 237-272, 2004.
20. Kimmel, R., Malladi, R. and Sochen, N. *Images as Embedded Maps and Minimal Surfaces: Movies, Color, Texture, and Volumetric Medical Images*, International Journal of Computer Vision, 39(2), pp. 111-129, 2000.
21. Maltret, J.-L. and Daniel, M. *Discrete curvatures and applications: a survey*, preprint, 2003.
22. Martin, R., *Estimation of principal curvatures from range data*, International Journal of Shape Modeling, 4:99-111, 1998.
23. Meek, D. and Walton, D. *On surface normal and gaussian curvature approximations given data sampled from a smooth surface*, Computer Aided Geometric Design, (17):521-543, 2000.
24. O'Neill, B. *Elementary Differential Geometry*, Academic Press, N.Y., 1966.
25. Saucan, E., Appleboim, E., Barak, E., Elber, G., Lev, R. and Zeevi, Y. Y. *Local versus Global in Quasiconformal Mapping for Medical Imaging*, in preparation.
26. Stokely, E. and Wu, S. Y. *Surface parameterization and curvature measurement of arbitrary 3d-objects: Five practical methods*, IEEE Transactions on Pattern Analysis and Machine Intelligence, volume 14(8), pp. 833-840, August 1992.
27. Sullivan, J. M. *Curvature Measures for Discrete Surfaces*, Preprint, 2002.
28. Surazhsky, T., Magid, E., Soldea, O., Elber, G., and Rivlin, E. *A Comparison of Gaussian and Mean Curvatures Estimation Methods on Triangular Meshes*, Proceedings of the IEEE International Conference on Robotics and Automation. Taipei, Taiwan, pp 1021-1026, September 2003.
29. Taubin, G. *Estimating the tensor of curvature of a surface from a polyhedral approximation*, ICCV, pp. 902-907, 1995.
30. Watanabe K. and Belyaev, A. G. *Detection of salient curvature features on polygonal surfaces*, EUROGRAPHICS 2001, volume 20, 2001.
31. Willmore, T. J. *Riemannian Geometry*, Clarendon Press, Oxford, 1993.
32. Yakoya, N. and Levine, M. *Range image segmentation based on differential geometry: A hybrid approach*, IEEE Transactions on Pattern Analysis and Machine Intelligence, volume 11(6), pages 643-649, June 1989.